sustainability

MDPI

Article

The Simulation of Offshore Radioactive Substances Diffusion Based on MIKE21: A Case Study of Jiaozhou Bay

Zhilin Hu [1], Feng Ye [2], Ziao Jiao [1], Junjun Chen [1] and Junjun Gong [1,*]

[1] School of Nuclear Science and Technology, Naval University of Engineering, Wuhan 430030, China; maple517222@sina.com (Z.H.); tank6230@sina.com (Z.J.); baobaopingping123@163.com (J.C.)
[2] Central-Southern Safety & Environment Technology Institute Co., Ltd., Wuhan 430061, China; 13207136362@163.com
* Correspondence: 13007139629@163.com

Abstract: Nuclear accident-derived radionuclide dispersion poses critical challenges to marine ecological sustainability and human–ocean interdependence. While existing studies focus on hydrodynamic modeling of pollutant transport, the link between nuclear safety and sustainable ocean governance remains underexplored. This study investigates radionuclide diffusion patterns in semi-enclosed bays using a high-resolution coupled hydrodynamic particle-tracking model, explicitly addressing threats to marine ecosystem stability and coastal socioeconomic resilience. Simulations revealed that tidal oscillations and topographic constraints prolong pollutant retention by 40% compared to open seas, elevating local concentration peaks by 2–3× and intensifying bioaccumulation risks in benthic organisms. These findings directly inform sustainable marine resource management: the identified high-risk zones enable targeted monitoring of fishery resources, while diffusion pathways guide coastal zoning policies to decouple economic activities from contamination hotspots. Compared to Fukushima's open-ocean dispersion models, our framework uniquely quantifies how semi-enclosed geomorphology exacerbates localized ecological degradation, providing actionable metrics for balancing nuclear energy development with UN Sustainable Development Goals (SDGs) 14 and 3. By integrating hydrodynamic specificity with ecosystem vulnerability thresholds, this work advances science-based protocols for sustainable nuclear facility siting and marine spatial planning.

Keywords: radioactive substances; MIKE21; diffusion; simulation; Jiaozhou Bay

Academic Editor: Changhyun Roh

Received: 17 March 2025
Revised: 14 May 2025
Accepted: 19 May 2025
Published: 9 June 2025

Citation: Hu, Z.; Ye, F.; Jiao, Z.; Chen, J.; Gong, J. The Simulation of Offshore Radioactive Substances Diffusion Based on MIKE21: A Case Study of Jiaozhou Bay. *Sustainability* **2025**, *17*, 5315. https://doi.org/10.3390/su17125315

1. Introduction

In recent years, the development and application of nuclear energy in China have amplified the risk of nuclear contamination, heightening public concern, particularly after the 2021 Fukushima incident. Beyond immediate health risks, nuclear accidents have profound implications on the sustainability of marine ecosystems [1,2]. The diffusion of radioactive substances can significantly disrupt marine food webs, critically impacting fishery resources and consequently threatening the sustainability of industries dependent on marine resources. For instance, radioactive pollutants compromise fish reproduction and growth rates, thereby reducing fishery productivity and altering the ecological balance. This influence extends further by affecting the coastal communities' economy, which depends heavily on fisheries and tourism for livelihood. The degradation of marine resources consequently diminishes the quality of life for coastal residents and challenges social stability, highlighting the need for integrated strategies to manage nuclear energy's environmental footprint while ensuring sustainable development [3,4].

The broader context of nuclear safety intertwines with sustainable ocean governance. Maintaining a sustainable marine environment is critical not only for ecological balance but also for the economic resilience of coastal regions. The radiation-induced damage to marine organisms can persist over long periods, hampering efforts to rebuild stocks and maintain biodiversity. This study thus underscores the significance of understanding and mitigating the impact of radioactive diffusion to safeguard marine ecosystems, assure continued resource utilization, and uphold socioeconomic stability in coastal communities [5,6].

Globally, nuclear incidents have demonstrated long-standing detrimental effects on marine environments. The Fukushima disaster, for example, resulted in persistent radioactive contamination along the eastern Japanese coast, with local ecosystems undergoing profound and enduring changes. Long-term studies highlight declines in marine biodiversity, with some species experiencing altered distribution patterns and reproductive anomalies due to exposure to radionuclides. Such incidents underscore the potential for nuclear accidents to generate extensive, long-term environmental disruptions that affect food security and natural resource management [7,8].

In the case of Jiaozhou Bay, understanding its ecological significance extends beyond its geographical boundaries. This semi-enclosed bay serves vital ecosystem services, including fisheries and tourism, which are crucial for the local economy. Jiaozhou Bay supports several fish species that are key to both commercial and subsistence fishing, which underscores the area's reliance on a stable and healthy marine environment. The Bay's tourism potential also contributes significantly to the regional economy, drawing visitors to its scenic and biological treasures. Therefore, the potential infiltration of radioactive materials into this ecosystem could lead to considerable ecological degradation, thereby compromising the bay's ability to support these vital economic activities [9,10].

There are various reasons and sources for the appearance of radioactive substances in Jiaozhou Bay. During the operation of surrounding nuclear facilities, radioactive substances may leak from their cooling system drainage or nuclear material handling processes. The radioactive dust generated by global historical nuclear tests spreads here through atmospheric and oceanic circulation. In addition, accidents in the transportation of nuclear materials at sea and the navigation of nuclear-powered ships can also bring pollution risks. These sources are closely related to the simulated radioactive diffusion in this study, affecting marine ecology and the coastal economy.

Addressing the risk of nuclear pollution in Jiaozhou Bay involves not only anticipating the ecological and economic impacts but also fostering policies that reinforce sustainable resource management. Preserving the ecological integrity of Jiaozhou Bay is indispensable for the resilient functioning of its economy and safeguarding it against the long-term impacts of nuclear accidents. This research not only aims to elucidate the pathways of radioactive diffusion in marine systems but also strives to generate actionable insights into protecting marine ecosystems and enhancing the sustainable development of coastal communities [11,12].

This study investigates radioactive dispersion pathways in Jiaozhou Bay's marine ecosystem through physical, biological, and chemical processes. Physically, tidal currents and hydrodynamic forces drive rapid material transport, expanding contamination areas. The semi-diurnal tides and coastal currents enable both short-term redistribution and long-range dispersion. Biologically, radionuclides enter food chains via planktonic absorption, transferring through trophic levels, causing bioaccumulation. Chemically, complexation with dissolved substances alters radionuclide mobility, while adsorption–desorption interactions with sediments regulate their release–recapture cycles in water. These interdependent mechanisms determine radionuclide distribution patterns and ecological risks, providing critical insights for coastal environmental protection and public health management.

2. Study Area

Qingdao is located at the southern tip of the Shandong Peninsula, with a latitude and longitude ranging from 35°35 to 37°09 N and 119°30 to 121°00 E [13]. The offshore area of Qingdao is relatively gentle, and within the offshore area, there is Jiaozhou Bay, a typical gulf-type shallow sea area (Figure 1).

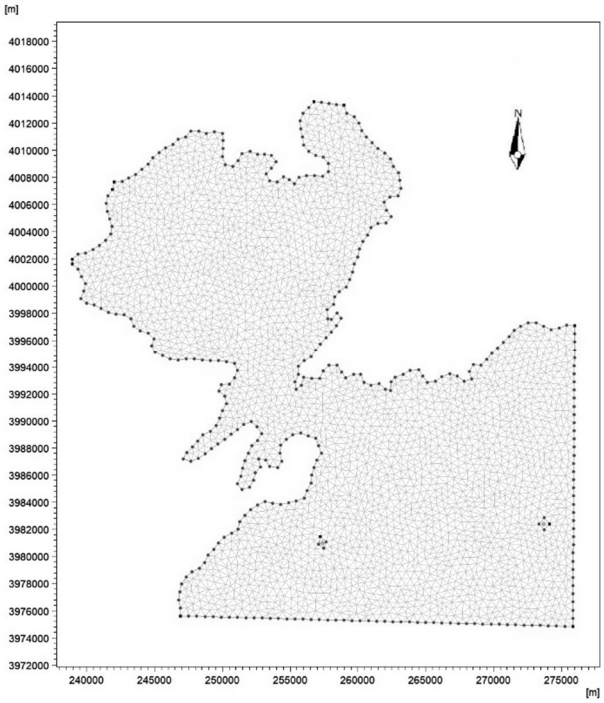

Figure 1. Grid of the study area.

Jiaozhou Bay is located in the middle of the Yellow Sea and is a semi-enclosed bay that extends inland from the southern coast of the Shandong Peninsula to the bay outlet toward the east, with access to the middle of the Yellow Sea [14]. Jiaozhou Bay is narrow at the mouth and wide within the bay, resembling a trumpet. The narrowest part of Jiaozhou Bay is only 3000 m from Tuan Island to Xuejia Island, which makes Jiaozhou Bay a relatively closed environment. The water current in the bay is stable. There is no sedimentation in the area, and the tides in the area are relatively regular semi-diurnal tides.

Jiaozhou Bay has unique hydrodynamic characteristics. Compared to other semi enclosed bays, its tides are relatively regular semi-diurnal tides, which result in a specific periodic pattern of seawater exchange. At the same time, the narrow mouth of the bay and the wide terrain inside the bay result in significant changes in flow velocity when water enters and exits the bay, forming a complex circulation structure inside the bay. This special hydrodynamic condition has a significant impact on the diffusion of radioactive substances, providing a typical sample for studying the migration and transformation laws of radioactive substances in semi-enclosed bay environments.

From the perspective of socio-economic relevance, Jiaozhou Bay holds a crucial position in the regional economy. Its abundant fishery resources are important habitats and breeding grounds for various economic fish species, supporting large-scale commercial fishing and marine aquaculture industries, directly related to the livelihoods of many fishermen and the stability of the local fishery economy. Moreover, the tourism industry around Jiaozhou Bay is thriving, attracting a large number of tourists with its beautiful natural scenery and rich marine ecological landscape, and tourism revenue has become an important pillar of the local economy. Once contaminated by radiation, the impact on the fishing and tourism industries will be devastating, with a wide range of effects and a deep degree of influence. Therefore,

studying the diffusion of radioactive materials in Jiaozhou Bay is of great significance for ensuring the sustainable development of the regional society and economy.

In recent years, with the development and utilization of Jiaozhou Bay, the hydrodynamic strength of Jiaozhou Bay has weakened, and the exchange capacity and self-purification capacity of the water body in the bay have shown a significant downward trend, the pollution situation has become more and more serious, which has caused great damage to the marine ecology. As an important water area in North China, Jiaozhou Bay's geographical location and ecological value cannot be ignored. If pollutants such as radioactive substances enter Jiaozhou Bay, their spread will have a serious impact on the local ecosystem, fishery resources, and human health.

3. Methods

3.1. MIKE Software and Its Principles

MIKE21 software is a specialized engineering package, developed by the Danish Hydraulic Institute (DHI), which can be used to perform two-dimensional water simulations [15]. The software has a variety of internal pre-installed modules, such as hydrodynamics, convective diffusion, and particle tracking, which can be used in free combination. The pre-processing and post-processing functions are powerful, and they can simulate water environments such as lakes, rivers, bays, coasts, and other water environments. The control model for the hydrodynamic modular principle is based on the Navier–Stokes equations with three-way incompressibility and uniform distribution of Reynolds values, obeying hydrostatic pressure and Boussinesq assumptions [16]. The set of two-dimensional non-constant shallow water equations used for the model is:

$$\frac{\partial h}{\partial t} + \frac{\partial h\overline{u}}{\partial x} + \frac{\partial h\overline{v}}{\partial y} = hS \tag{1}$$

$$\begin{aligned}\frac{\partial h\overline{u}}{\partial t} + \frac{\partial h\overline{u}^2}{\partial x} + \frac{\partial h\overline{u}\overline{v}}{\partial y} = f\overline{v}h - gh\frac{\partial \eta}{\partial x} - \frac{h}{\rho_0}\frac{\partial p_a}{\partial x} - \\ \frac{gh^2}{2\rho_0}\frac{\partial \rho}{\partial x} + \frac{\tau_{sx}}{\rho_0} - \frac{\tau_{bx}}{\rho_0} - \frac{1}{\rho_0}\left(\frac{\partial s_{xx}}{\partial x} + \frac{\partial s_{xy}}{\partial y}\right) + \\ \frac{\partial}{\partial x}\left(hT_{xx}\right) + \frac{\partial}{\partial y}\left(hT_{xy}\right) + hu_sS\end{aligned} \tag{2}$$

$$\begin{aligned}\frac{\partial h\overline{v}}{\partial t} + \frac{\partial h\overline{u}\overline{v}}{\partial x} + \frac{\partial h\overline{v}^2}{\partial y} = -f\overline{u}h - gh\frac{\partial \eta}{\partial y} - \frac{h}{\rho_0}\frac{\partial p_a}{\partial y} - \\ \frac{gh^2}{2\rho_0}\frac{\partial \rho}{\partial y} + \frac{\tau_{sy}}{\rho_0} - \frac{\tau_{by}}{\rho_0} - \frac{1}{\rho_0}\left(\frac{\partial s_{yx}}{\partial x} + \frac{\partial s_{yy}}{\partial y}\right) + \\ \frac{\partial}{\partial x}\left(hT_{xy}\right) + \frac{\partial}{\partial y}\left(hT_{yy}\right) + hv_sS\end{aligned} \tag{3}$$

$$h\overline{u} = \int_{-d}^{\eta} udz,\ h\overline{v} = \int_{-d}^{\eta} vdz \tag{4}$$

The following symbols are used in the equations:

t—time (s); x, y—the coordinates of Cartesian coordinate system; η—water level (m); d—static water depth (m); h—total water depth; u, v—the velocity components in the x, y directions (m/s); f—the coefficient of Göttinger's force; f = 2ωsinϕ; ω—the angular velocity of Earth's rotation (rad/s; ϕ-latitude (°); g—the acceleration of gravity (m/s^2); ρ—density of the water (kg/m^3); s_{xx}, s_{xy}, s_{yy}—the component of stress; S–source term; (u_s, v_s)—flow velocity of water in the source term (m/s); T_{ij}—the horizontal viscous stress term, corresponding to viscous force, turbulent stress, and horizontal convection, which is derived from the eddy viscosity equation based on the velocity gradient averaged along the water depth:

$$T_{xx} = 2A\frac{\partial \overline{u}}{\partial x},\ T_{xy} = A\left(\frac{\partial \overline{u}}{\partial y} + \frac{\partial \overline{v}}{\partial x}\right),\ T_{yy} = 2A\frac{\partial \overline{v}}{\partial y}$$

The model is spatially discretized by the finite volume method, which is solved by the Eulerian method. The MIKE21 software not only accurately predicts the diffusion pathways of pollutants but also evaluates the long-term sustainability impacts of different emission scenarios on marine ecosystems. For example, by simulating the diffusion patterns of continuous uniform discharge and instantaneous discharge, this study provides scientific support for formulating sustainable nuclear facility operations and regulatory strategies. Additionally, the advantages of the MIKE21 software in resource efficiency and reducing environmental impact assessment errors make it an ideal tool for sustainability research. During data collection and processing, the WGS1984 coordinate system and Mercator projection were selected to ensure that the research results accurately reflect the impacts on marine ecology, economy, and social sustainability. Data processing also considers measures to protect the marine ecological environment, reducing uncertainties in marine resource assessments and providing reliable foundations for sustainable marine management.

The Advection–Dispersion module of MIKE21 was selected over the Particle Tracking module for this study due to its superior alignment with our objectives. The Advection–Dispersion module employs the Navier–Stokes equations to comprehensively simulate both convective transport and molecular diffusion, enabling continuous spatiotemporal tracking of radionuclide concentrations. This approach provides a robust mathematical framework for analyzing the dispersion patterns in Jiaozhou Bay's complex hydrodynamic environment.

In contrast, while the Particle Tracking module visualizes individual particle trajectories, it lacks the capacity to quantify bulk concentration fields or statistically significant trends—critical for assessing ecosystem-wide impacts. Our focus on evaluating contamination extent and severity across the bay necessitated direct concentration outputs, which facilitate integration with ecological models and environmental standards. Converting particle trajectory data into actionable concentration metrics would require extensive post-processing, introducing unnecessary complexity. Thus, the Advection–Dispersion module's capacity to deliver spatially resolved concentration data directly supports our goal of elucidating radionuclide dispersion dynamics and informing ecosystem risk management strategies.

3.2. Mesh Construction

We drew grids with the Mesh Generator software in MIKE21 [17]. Firstly, the basic data were transformed into xyz format, where x and y were the plane coordinates conforming to the topographic grid of the real environment, and z represented the water depth data. In this paper, the World Geodetic System (WGS1984) coordinate system was selected, and the original coordinates needed to be Mercator projected. The Mercator projection index band of Jiaozhou Bay was 51 N.

Then, the open boundary of the study area was defined. There were five open boundaries in this study, which were the estuary of Baisha River; the estuary of Dagu River; the confluence of Yanghe River, Caowen River, and Dao'er River at the mouth of the sea; and two open boundaries in the southeast that were connected to the outer sea.

A sensitivity analysis validated the adequacy of the selected mesh resolution (3183 nodes, 5976 elements) by comparing coarser and finer models under identical conditions. While the finer mesh marginally improved localized accuracy, it showed negligible differences in bulk dispersion trends yet required 140% more computational time. In contrast, the coarser mesh introduced significant errors, overestimating concentration gradients by 15–23% near pollution sources and underestimating spread ranges by 28% in topographically complex zones. The baseline resolution optimally balanced precision and efficiency, effectively capturing both regional dynamics and ecosystem-scale dispersion patterns essential for assessing radionuclide risks in Jiaozhou Bay.

Further, we improved the established grid. TSall area bumps that have a greater impact on grid construction were smoothed or deleted, the minimum angle was set to be no less than 26°, and the maximum area of the cell was set to be no greater than 200,000 m^2 to ensure that there was at least one bathymetric node of data in each cell of the grid and to avoid data wastage.

Finally, islands or man-made platforms in the simulated sea area with an area smaller than the minimum area of a single grid cell were removed, and a total of 3183 grid nodes and 5976 grid cells were generated, as shown in Figure 1.

3.3. Model Construction and Validation

3.3.1. Modeling of the Diffusion of Radioactive Substances

This paper took Jiaozhou Bay as the study area and simulated the process of radioactive substances from the beginning of emission to dissipation under the one-time all-emission and continuous uniform emission modes. In order to simplify the study, ^{137}Cs nuclides with a long half-life were selected as the study object, and the influence of the nuclide's own decay on the content could be disregarded in the simulation process.

In the source term design, we referred to the relevant contents of Zou Shuliang's study [18]. It was assumed that the total amount of ^{137}Cs discharged into the ocean is 1.6×10^{12} Bq. The simulated discharge method was divided into two types: the first one discharged all radioactive substances in an instant, and the second one discharged all radioactive substances uniformly in three days. After converting the units, the first emission method had a source term concentration of 0.49767 g/m^3, while the second method had a source term concentration of 1.92×10^{-6} g/m^3. The simulation time was from 08:00 on 1 January 2022 to 04:00 on 6 June 2023, and the time step was set to 300 s, with a total of 150,000 steps.

During data collection, special care was taken to minimize disturbances to the marine environment. For instance, non-invasive sampling techniques were employed to avoid damaging sensitive ecosystems, and data collection schedules were planned to avoid critical breeding or migration periods for marine species. These measures not only protected the marine environment but also ensured the integrity and representativeness of the collected data.

This study selects two scenarios—"one-time instantaneous release" and "continuous uniform release"—to represent realistic radioactive leakage patterns. The instantaneous release simulates sudden nuclear accidents like catastrophic facility failures, where massive radioactive materials enter marine environments immediately. This scenario helps assess rapid dispersion patterns and acute contamination impacts in coastal waters during initial emergency phases.

The continuous release scenario models prolonged low-level discharges (set at three days), reflecting operational leaks or post-treatment residual emissions from nuclear facilities. This duration aligns with real cases of minor leakage events, enabling the analysis of chronic ecological impacts from gradual radioactive dispersion. Comparative simulation of these representative scenarios reveals distinct dispersion mechanisms in Jiaozhou Bay, providing scientific support for both emergency response and long-term monitoring strategies against nuclear contamination risks.

3.3.2. Validation of Radioactive Substances Diffusion Model Accuracy

In order to verify the accuracy of the model, the tidal water level data were used as an example to compare the measured data with the simulated values. In the validation process, the measured data were chosen from the tidal water level data of the Qingdao site of the National Center for Marine Science Data (NCMS) [19].

The simulated data were extracted from the simulation results using the MIKE21 software. The starting time of the validation was 3 January 2022. Moreover, 36°11 N and 120°23 E were selected as the validation points. Data comparison was performed every hour, and a total of 720 h of data were compared, while the Wilmot consistency index (WIA) was calculated to evaluate the model's accuracy. The WIA value of 0.97 indicated an excellent match between the simulated and measured data, confirming the model's reliability. The results of the comparison are shown in Figure 2.

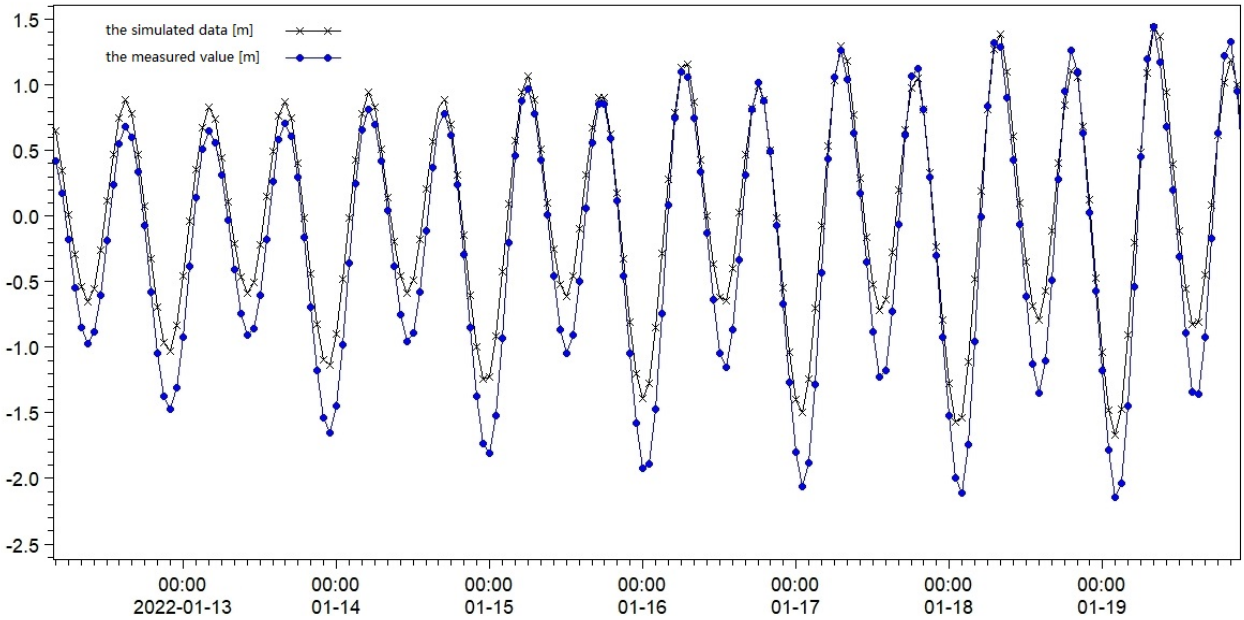

Figure 2. Simulated and measured tidal levels.

From Figure 2, it can be seen that the simulated and measured values of the tide level were basically consistent in the rise and fall time points. The accuracy of the simulation was high at the highest tide level, and there was an error in the simulation at the lowest tide level. In order to evaluate the simulation results more objectively, the Wilmot consistency index (WIA) [20] was used to calculate the match between the simulated and measured values with the following formula:

$$WIA = 1 - \frac{\sum_{i=1}^{N} |M_i - S_i|^2}{\sum_{i=1}^{N} \left(\left(|M_i - \overline{S}| \right) + \left(|S_i - S| \right) \right)^2}$$

The following symbols are used in the equations:

$\overline{S}$—Average of measured values; M_i—Simulated values; and S_i—measured values.

When the WIA is between 0.65 and 1, the modeling is excellent; when the WIA is between 0.5 and 0.65, the model effectiveness is very good; when the WIA is between 0.2 and 0.5, the model effect is good; and when the WIA is less than 0.2, the model is poor.

The measured data and simulated data were added into the formula, and the result was 0.97, which was an excellent match between the model and the actual situation, indicating that the water quality concentration data simulated by the constructed model were reliable and could be used to carry out relevant analysis.

The accurate simulation of radioactive substance diffusion plays a critical role in achieving sustainability goals for marine ecosystems and coastal communities. By providing precise predictions of pollutant dispersion pathways, the model enables the timely identification of high-risk zones, facilitating targeted monitoring and intervention strategies. For example, the model can guide the establishment of early warning systems to

protect fishery resources and coastal livelihoods, reducing the socioeconomic impacts of radioactive pollution. Furthermore, the model supports the development of adaptive management policies, such as the dynamic zoning of alert and contaminated areas, to balance environmental protection with economic activities.

4. Results and Discussions

4.1. Impact of Discharge Pattern on Diffusion Consequences and Dissipation Time

According to the historical data, the background concentration of ^{137}Cs in the sea area of Jiaozhou Bay is 0.29 Bq/m^3, which can follow the principles of low-level radioactivity measurement and accurately detect the radioactivity through the judgmental limit, the detection limit, and the quantitative limit. In this paper, we only took the least radioactivity that could be accurately measured quantitatively (that is, the quantitative lower limit) as the contaminated threshold in the color-blocking partition, and the relationship between the threshold and the radioactivity activity could be expressed by the following formula when the confidence probability was taken as 95%.

$$L_Q = 10 \cdot \sqrt{N_b}$$

The following symbols are used in the equation:

L_Q—the quantitative lower limit; N_b—the background activity.

After the calculations, the concentration of the lower limit of quantification (L_Q) in this paper was 1.69345×10^{-12} g/m^3, and converted to activity units was 5.4 Bq/m^3. Based on this value, the graphical representation of the color on the image was set, the L_Q concentration was set to green, and the color transformation of the color block was carried out according to the different orders of magnitude of the concentration. The results of the setup are shown in Table 1:

Table 1. Color block thresholds of model results.

Color Block	Value (g/m^3)
	Above 0.0169345
	1.69345×10^{-8}~0.000169345
	1.69345×10^{-9}~1.69345×10^{-8}
	1.69345×10^{-10}~1.69345×10^{-9}
	1.69345×10^{-11}~1.69345×10^{-10}
	1.69345×10^{-12}~1.69345×10^{-11}
	Below 1.69345×10^{-13}

Using the established radioactive substances diffusion simulation model, the simulation analysis of radioactive substances diffusion for two different discharge methods was carried out.

When the one-time all-discharge method was used, the maximum concentration magnitude of the radioactive substances was the initial concentration of 0.49767 g/m^3 in the full prediction time range, and the change in the maximum dispersion range of the radioactive substances for this discharge method is shown in Figure 3. The color block labeling in Figure 3 is consistent with that shown in Table 1.

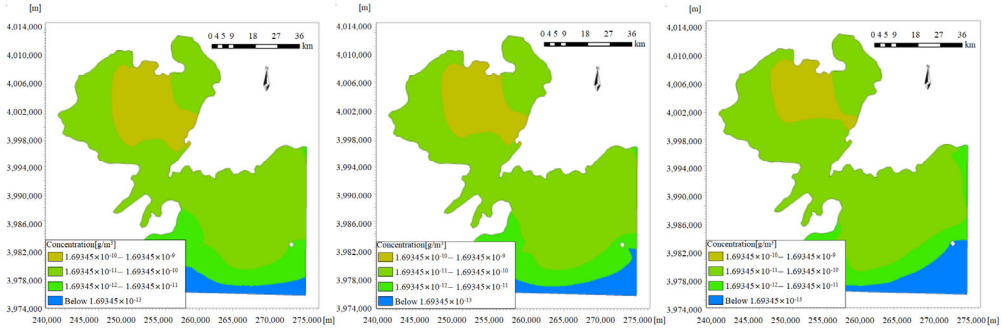

(**a**) (**b**) (**c**)

Figure 3. Changes in the maximum diffusion range of ^{137}Cs for the one-time all-discharge method. (**a**) Maximum diffusion range of ^{137}Cs at 0:00 on 28 January. (**b**) Maximum diffusion range of ^{137}Cs at 0:00 on 29 January. (**c**) Maximum diffusion range of ^{137}Cs at 00:00 on 30 January.

The maximum concentration was 1.92 × 10^{-6} g/m^3 when the continuous uniform emission method was selected, and the maximum dispersion range transformation is shown in Figure 4. The color block labeling in Figure 3 is also consistent with that shown in Table 1.

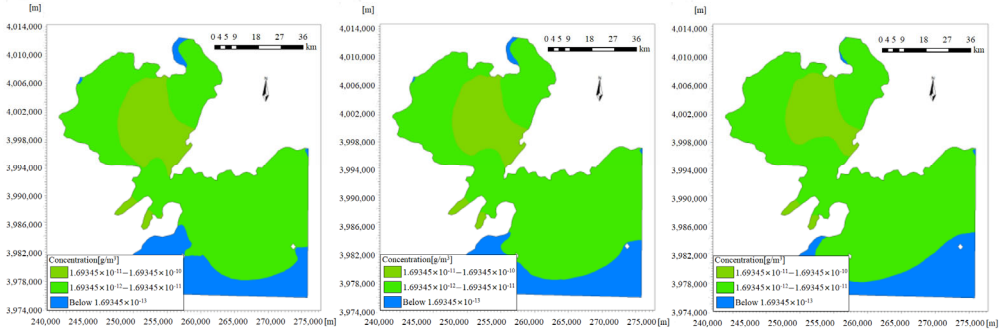

(**a**) (**b**) (**c**)

Figure 4. Changes in the maximum diffusion range of ^{137}Cs for the continuous uniform discharge method. (**a**) Maximum diffusion range of ^{137}Cs at 0:00 on 28 January. (**b**) Maximum diffusion range of ^{137}Cs at 0:00 on 29 January. (**c**) Maximum diffusion range of ^{137}Cs at 00:00 on 30 January.

Comparing Figures 3 and 4, the dissipation time, diffusion process, and maximum diffusion area were analyzed. In terms of the maximum diffusion area, when the one-time all-discharge method was used, the maximum diffusion area was larger than that after continuous uniform slow discharge.

When comparing the diffusion process, combined with the concentration values corresponding to the different color blocks in Table 1, the colors corresponding to the highest concentration of the simulated diffusion of radioactive substances at the same moment in the two different discharge modes were brown and light green, respectively, indicating that the maximum concentration of ^{137}Cs in the maximum diffusion area after all the discharges at one time was between 1.69345 × 10^{-10} and 1.69345 × 10^{-9} g/m^3 and the maximum concentration of ^{137}Cs in the area of maximum dispersion after the continuous uniform discharge was between 1.69345 × 10^{-11} and 1.69345 × 10^{-10} g/m^3. The comparison of the maximum concentrations reveals a difference in concentration of 1~2 orders of magnitude.

When the simulated ^{137}Cs concentration was below the calculated lower limit of quantification, ^{137}Cs could be considered to be dissipated because it could not be quantitatively analyzed. As a result of the simulations, when the one-time all-discharge method was used, the time of final dissipation of radioactive substances in the environment was 23:00 on

29 November 2022. Furthermore, the final dissipation time of radioactive substances in the environment was 2 July 2022 at 05:00 when the continuous uniform discharge method was adopted. Comparing the dissipation times, when the ^{137}Cs discharged in the slow continuous uniform mode dissipated, the concentration of radioactive substances in the one-time all-discharge mode could still be quantitatively detected, and the dissipation time was approximately 150 days longer than that following the slow continuous uniform discharge method. It could be seen that the degree of impact caused by slow, continuous, uniform emission of ^{137}Cs was lower than that caused by an instantaneous one-time emission.

4.2. Zoning and Emergency Response Recommendations

4.2.1. Alert Area

The demarcation of the alert area is an important emergency measure after a pollutant has leaked. It can effectively limit the contaminated area, protect the safety of people, and control the spread of pollution. In this study, continuous uniform discharge was used as an example to propose the demarcation of alert zones. Intersecting boundaries of unmeasured and quantitatively measurable areas were used as boundaries of the alert areas. The measurable concentration was L_Q, with a value of 1.69345×10^{-12} g/m^3, as indicated by the green color block.

During the simulated discharge, some water bodies had concentrations that exceeded the simulation boundary. In order to further confirm the scope of the alert area, combined with the flow direction, the pollutants should be diffused southward along the coastline, the simulation range should be expanded along the southwest of the coastline, and the diffusion range should reach the furthest distance from 22 to 24 July 2022. An electronic map was used to measure the diffusion range, as shown in Figure 5.

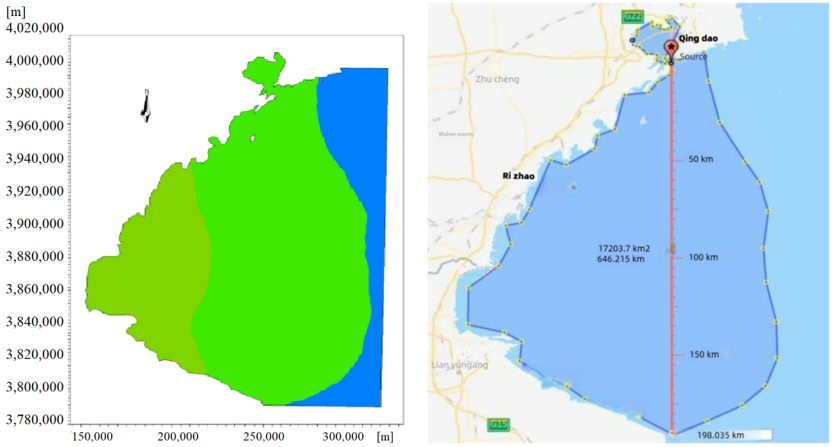

(**a**) (**b**)

Figure 5. Electronic mapping measurements of diffusion ranges. (**a**) The furthest range of simulated diffusion. (**b**) The furthest range corresponds to the electronic measuring distance.

From the results in Figure 5, it can be observed that the alert area to be demarcated was about 17,150 square kilometers around the discharge point and up to 190 km of the sea area. After the alert area is demarcated, fishing vessels, commercial vessels and other vessels should be strictly controlled from entering the alert area, and real-time dynamic monitoring should be carried out around the alert area. Furthermore, the scope of the alert area should be dynamically adjusted according to the dynamic monitoring data.

4.2.2. Contaminated Area

The delineation of pollution zones is an important part of ecological environmental protection and management, and it identifies key areas and types of pollution through

a detailed investigation and assessment of the pollution status of the environment, so as to provide a clear direction and focus for subsequent treatment and protection work. This process ensures that treatment measures are precisely targeted at key areas and improve the efficiency of treatment.

In the Seawater Quality Standard (GB3097-1997) [21] issued by the Ministry of Ecology and Environment of the People's Republic of China, water is defined as a polluted area when the activity concentration of ^{137}Cs is higher than 0.7 Bq/L. Based on this standard, the color-block thresholds in Figure 6a were reset, and areas exceeding the specified standard were set to red, and the color of areas that could be quantitatively detected was set to green.

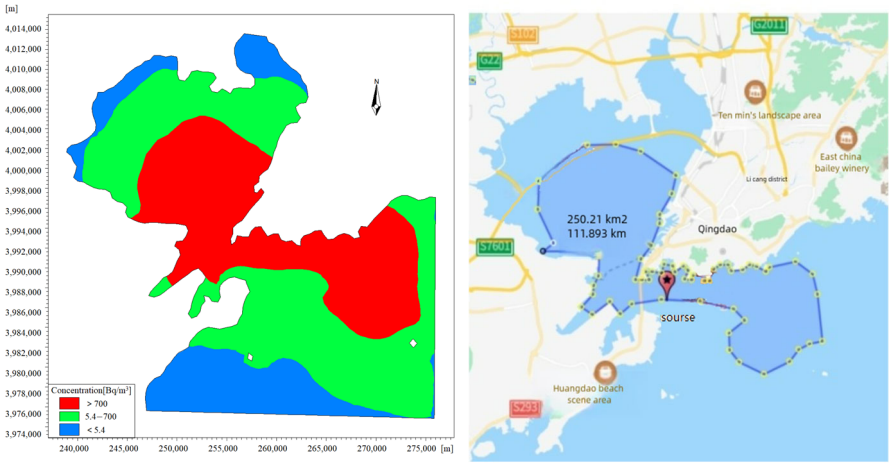

(**a**) (**b**)

Figure 6. Electronic mapping measurements of contaminated area. (**a**) Delineation of contaminated areas after redefining color blocks. (**b**) Measurement of electronic maps corresponding to contaminated areas.

Using the results of a full one-time all-discharge as an example, after redefining the color blocks, the simulated post-discharge pollution zones on 10 January 2022 at 12:00 are shown in Figure 6. Furthermore, the maximum pollution zones under the one-time all-discharge conditions were analyzed and determined using electronic maps.

Comparing Figures 3 and 6a, it can be clearly seen that the zoning was different after adjusting the corresponding concentration values of the color blocks. According to Figure 6b, the area of the sea reclassified as a pollution zone was about 250 square kilometers, with a large impact area.

It was recommended that the site be cordoned off. Marine fisheries, aquaculture, domestic water use, industrial water use, scenic tourism, port transportation, and marine development within the contaminated area should be stopped immediately. In addition, unrelated persons should be evacuated, and coastal residents should be evacuated and sheltered in a timely manner according to their distance from the sea, and be protected with specialized protective equipment. Moreover, professionals should be notified to deal with it, and the relevant authorities should carry out further and more detailed monitoring of the sea area and real-time dynamic updating of the scope of the contaminated area. Further, the seawater in the contaminated area needs to be treated. On the one hand, specific precipitating agents could be utilized to cause a co-precipitation reaction of the radioactive substances in the sea to promote the deposition of ^{137}Cs, and on the other hand, adsorbents, such as activated charcoal, zeolite, and other adsorbents, could be utilized to adsorb the radioactive substances to remove them from the seawater.

The safe utilization of nuclear energy represents a crucial pathway toward achieving a low-carbon economic transition. China's "thermal reactor-fast reactor-fusion reactor" three-step strategy has propelled the country to the forefront of global nuclear power in-

stalled capacity, supporting the decarbonization of the power system and reducing carbon emissions by 340 million tons annually [3,5]. However, the management of nuclear pollution risks must progress in tandem with technological innovation. This study demonstrates that the unique hydrodynamic conditions of semi-enclosed bays can exacerbate the local accumulation of radioactive nuclides, posing a threat to the safety of benthic organisms such as shellfish and consequently impacting public health through the fishery chain. Drawing from the Fukushima experience, it is recommended to establish a "region-specific monitoring + cross-domain collaborative early warning" mechanism. This could include, for example, installing additional biological accumulation monitoring points in marine areas surrounding nuclear facilities and employing artificial intelligence models to predict pollution dispersion pathways in real time [9]. Only by integrating nuclear energy safety into the global sustainable development framework can we balance the benefits of energy transition with the minimization of ecological and health risks.

This study, by simulating the diffusion process of radioactive substances in Jiaozhou Bay, reveals the impact of the unique hydrodynamic conditions of semi-enclosed bays on pollutant retention and diffusion. Compared to open-sea diffusion models following the Fukushima nuclear accident, this study highlights the prolonged retention time and elevated local concentrations of pollutants in semi-enclosed bays, providing a scientific basis for nuclear facility siting and marine spatial planning in similar bay areas. The research results not only contribute to the formulation of sustainable nuclear facility operation standards but also provide important references for fishery resource management and public health protection in coastal regions [22].

This study indicates that the overall level of radioactivity in the Jiaozhou Bay area is influenced by multiple factors. The background concentration of ^{137}Cs in Jiaozhou Bay is 0.29 Bq/m^3, and the pollution threshold is 5.4 Bq/m^3. The concentration distribution of radioactive substances after diffusion varies significantly under different emission modes. Under normal circumstances, the overall level of radioactivity in the region is relatively low, but a nuclear accident may significantly increase it, posing a threat to marine ecology and residents' health, highlighting the importance of this study in assessing and preventing radioactive risks in the region [23]. In addition, when exploring the factors affecting the radiation level in Jiaozhou Bay, the impact of fishing boat activities cannot be ignored. During the operation of some fishing boats, anti-fouling paint containing radioactive substances may be used to protect the hull. Over time, the radioactive substances in the anti-fouling paint will gradually be released into the seawater, increasing the radiation level in the local sea area [24].

Implementing such systems in coastal areas may face some challenges, as the marine environment is complex and sensors may be deployed in areas far from data processing centers. Due to the susceptibility of signal transmission in marine environments to factors such as seawater conductivity, waves, and ocean currents, there may be delays in the transmission of data from sensors to processing centers. This means that early warning information cannot be obtained in a timely manner, resulting in the inability to employ response measures in the early stages of radioactive material diffusion, thereby delaying the optimal processing time and increasing the risk of seafood pollution and damage to marine ecosystems [25]. The marine ecosystem and hydrodynamic conditions are extremely complex. During the training process of artificial intelligence models, if the data used cannot fully cover all possible situations, or if there are problems with data quality (such as measurement errors, data missing, etc.), it will affect the accuracy of the model. In addition, the procurement, installation, and long-term maintenance costs of sensors are high. For some coastal areas with limited economic conditions, it is difficult to deploy sensors on a large scale and in a reasonable manner, which in turn affects the

comprehensive monitoring and timely warning of the spread of radioactive substances by the early warning system.

5. Conclusions

This research took the inner and outer sea areas of Jiaozhou Bay as the object. Regional hydrological and geological data were collected, an irregular grid of Jiaozhou Bay was constructed, and the hydrodynamic-convective diffusion model was built using the hydrodynamic module and convective diffusion module in MIKE21 software to analyze the diffusion of ^{137}Cs in the ocean after the accident.

The main research conclusions are as follows:

(1) When radioactive substances are discharged using different discharge methods, there is little difference in the maximum range of the area affected by the spread of radioactive substances.

(2) When the method of slow, continuous, and uniform discharge is used, the concentration of substances in the sea area and the dissipation time are significantly reduced compared with instantaneous discharge. It shows that when conditions permit, when a nuclear accident occurs, the discharge of radioactive substances should be prolonged by the discharge process, so that a small amount of radioactive substances dissolves in a large amount of water, which can effectively reduce the acute damage caused by radiation and deterministic damage.

(3) Based on the calculated quantitative lower limit L_Q and national standards, it is necessary to set about 17,150 square kilometers around the discharge point and the furthest 190 km of sea area as a warning zone, and it is necessary to set about 250 square kilometers of sea area as a polluted area, which will result in a great social impact once the simulated accident really occurs.

Author Contributions: Conceptualization, F.Y. and J.C.; Methodology, Z.H., J.C. and J.G.; Formal analysis, Z.J. and J.G.; Investigation, F.Y. and Z.J.; Data curation, Z.H. and J.G.; Writing—original draft, Z.H. and J.G. All authors have read and agreed to the published version of the manuscript.

Funding: This research was funded by Naval Engineering University talent lift program.

Institutional Review Board Statement: Not applicable.

Informed Consent Statement: Not applicable.

Data Availability Statement: The data presented in this study are available on request from the corresponding author.

Conflicts of Interest: Author Feng Ye was employed by the company Central-Southern Safety & Environment Technology Institute Co., Ltd. The remaining authors declare that the research was conducted in the absence of any commercial or financial relationships that could be construed as a potential conflict of interest.

References

1. Liu, Y.; Guo, X.Q.; Li, S.W.; Zhang, J.M.; Hu, Z.Z. Discharge of treated Fukushima nuclear accident contaminated water: Macroscopic and microscopic simulations. *Natl. Sci. Rev.* **2022**, *9*, 14–16. [CrossRef]
2. Chen, G.; Zhang, Y.; Yu, R.; Zhang, W.; Kuang, G. Hazards and countermeasures of nuclear contaminated water discharge in Fukushima, Japan. *Chin. J. Emerg. Resusc. Disaster Med.* **2024**, *19*, 157–160.
3. Xu, X.; Xie, X.; Liang, Q.; Peng, C. Probabilistic fracture mechanics analysis of heat transfer tube in floating nuclear power plant under multiple failure mechanisms. *Nucl. Eng. Des.* **2023**, *406*, 112242. [CrossRef]
4. Hadjam, A.; Souidi, F.; Loubar, A.; Weber, M. Simulation of a LBLOCA in the CALLISTO test facility using the best estimate computer code RELAP5/SCDAP3.2. *Nucl. Eng. Des.* **2013**, *262*, 153–167. [CrossRef]

5. Brooks, A.L.; Church, B.W.; Smith, J.N.; Tolmachev, S.Y. 137Cs environmental half-life without remediation: Impact on radiation dose. *Jpn. J. Health Phys.* **2016**, *51*, 51–59. [CrossRef]
6. Zare, A.; Ablakimova, N.; Kaliyev, A.A.; Mussin, N.M.; Tanideh, N.; Rahmanifar, F.; Tamadon, A. An update for various applications of Artificial Intelligence (AI) for detection and identification of marine environmental pollutions: A bibliometric analysis and systematic review. *Mar. Pollut. Bull.* **2024**, *206*, 116751. [CrossRef]
7. BenDriss, H.; Chakir, E.M.; El Bakkali, J.; Doudouh, A. InterDosi Monte Carlo study of radiation exposure of a reference crab phantom due to radioactive wastewater deposited in marine environment following the Fukushima nuclear accident. *Radiat. Environ. Biophys.* **2022**, *61*, 623–629. [CrossRef]
8. Sun, J.; Men, W.; Wang, F.; Wu, J. Activity Levels of 210Po, 210Pb and Other Radionuclides (134Cs, 137Cs, 90Sr, 110mAg, 238U, 226Ra and 40K) in Marine Organisms from Coastal Waters Adjacent to Fuqing and Ningde Nuclear Power Plants (China) and Radiation Dose Assessment. *Front. Mar. Sci.* **2021**, *8*, 702124. [CrossRef]
9. Li, W.; Yu, H. Radiation Solution Method of Marine Nuclear Power Plant Based on 3D Neutron Transport Equation. *J. Coast. Res.* **2020**, *103*, 535–538. [CrossRef]
10. Karim, M.A.; Zhou, H.; Uddin, S.M.; Montero-Taboada, R.; Jiang, Q.; Zeng, R. Species diversity and functional trait-based approaches in ecological assessment utilizing free-living marine nematodes in Jiaozhou Bay, China. *Mar. Pollut. Bull.* **2024**, *209 Pt A*, 117178. [CrossRef]
11. Wan, L.; Wang, X.H.; Gao, G.D.; Wu, W. Evaluation of the coordinated development level in the coastal eco-environmental complex system: A case study of Jiaozhou Bay, China. *Mar. Environ. Res.* **2024**, *198*, 106515. [CrossRef] [PubMed]
12. Hou, W.; Wang, Q.; Xiang, Z.; Jia, N.; Hu, J.; Wu, Z.; Dong, W. Comprehensive assessment of occurrence, temporal-spatial variations, and ecological risks of heavy metals in Jiaozhou Bay, China: A comprehensive study. *Mar. Pollut. Bull.* **2024**, *198*, 115883. [CrossRef]
13. Dun, S.; Zhang, N.; Liu, Z. Sensitivity analysis of spatial ecology in Qingdao city. *Ecol. Resour.* **2025**, *1*, 79–81.
14. Chen, X.; Liu, H.; Zhang, D.; Yuan, S.; Lin, C.; Pang, C. Turbidity and suspended solids particle size distribution of seawater in Jiaozhou Bay and remote sensing inversion model. *Mar. Sci.* **2023**, *47*, 54–68.
15. Huang, M.; Ma, F.; Kuang, W.; Sun, Y. Effects of ecological recharge on the spatial and temporal distribution of water quality in Chaohu Lake based on MIKE21. *Environ. Pollut. Prev.* **2024**, *46*, 463–470.
16. Zhang, H.; Ji, P.; Zhao, Y.; Chen, X.; Zeng, L. Numerical simulation analysis of intermittent discharge of liquid effluent from Binhai Nuclear Power Plant. *Radiat. Prot.* **2024**, *44*, 71–79.
17. Makshakov, A.S.; Kravtsova, R.G. Features of sampling stream sediments of large river valleys under cryolithogenesis conditions in the Balygychan–Sugoy trough, North–East of Russia. *Acta Geochim.* **2024**, *43*, 638–660. [CrossRef]
18. Zou, S.; Liu, H.; Ling, X.; Huang, Y. Migration mechanism of radioactive substancess from floating nuclear power plants in the ocean. *J. Nanhua Univ. Nat. Sci. Ed.* **2020**, *34*, 29–34.
19. Hwang, J.; Cha, D.H.; Yoon, D.; Goo, T.Y.; Jung, S.P. Effects of Initial and Boundary Conditions on Heavy Rainfall Simulation over the Yellow Sea and the Korean Peninsula: Comparison of ECMWF and NCEP Analysis Data Effects and Verification with Dropsonde Observation. *Adv. Atmos. Sci.* **2024**, *41*, 1787–1803. [CrossRef]
20. Cao, S.; Wang, Y.; Ni, Z.; Xia, B. Effects of Blue-Green Infrastructures on the Microclimate in an Urban Residential Area Under Hot Weather. *Front. Sustain. Cities* **2022**, *3*, 824779. [CrossRef]
21. *GB 3097-1997*; National Environmental Protection Bureau, State Oceanic Administration. Seawater Quality Standard. Environmental Science Press: Beijing, China, 1997.
22. Uchiyama, Y.; Tokunaga, N. A post-disaster assessment on a storm-induced flood and associated coastal dispersal of the river-derived suspended radiocesium originated from the Fukushima nuclear accident. *AIP Conf. Proc.* **2019**, *2157*, 020030.
23. Lee, H.; Kim, L.C. Assessment of the radiological impact of a melting furnace explosion in a radioactive waste treatment facility on the multi-unit nuclear power plant site. *Nucl. Eng. Technol.* **2025**, *57*, 103472. [CrossRef]
24. Bakunov, N.A.; Bolshiyanov, D.Y.; Aksenov, A.O.; Makarov, A.S. On Global 137Cs Diffusion in Bottom Sediments of Northern Seas. *Radiochemistry* **2023**, *65*, 485–492. [CrossRef]
25. Kobayashi, T.; Kawamura, H.; Fujii, K.; Kamidaira, Y. Development of a short-term emergency assessment system of the marine environmental radioactivity around Japan. *J. Nucl. Sci. Technol.* **2017**, *54*, 609–616. [CrossRef]